

Gravitational Redshift of Galaxies in Clusters from the Sloan Digital Sky Survey and the Baryon Oscillation Spectroscopic Survey

Iftach Sadeh,^{*} Low Lerh Feng,[†] and Ofer Lahav[‡]

*Astrophysics Group, Department of Physics and Astronomy,
University College London, Gower Street, London WC1E 6BT, United Kingdom*

(Dated: October 20, 2014)

The gravitational redshift effect allows one to directly probe the gravitational potential in clusters of galaxies. Following up on Wojtak *et al.* [Nature (London) 477, 567 (2011)], we present a new measurement. We take advantage of new data from the tenth data release of the Sloan Digital Sky Survey and the Baryon Oscillation Spectroscopic Survey. We compare the spectroscopic redshift of the brightest cluster galaxies (BCGs) with that of galaxies at the outskirts of clusters, using a sample with an average cluster mass of $10^{14} M_{\odot}$. We find that these galaxies have an average relative redshift of -11 km/s compared with that of BCGs, with a standard deviation of $+7$ and -5 km/s. Our measurement is consistent with that of Wojtak *et al.* However, our derived standard deviation is larger, as we take into account various systematic effects, beyond the size of the dataset. The result is in good agreement with the predictions from general relativity.

INTRODUCTION

The gravitational redshift (GRS) effect in clusters of galaxies is a feature in any metric theory of gravity. It is caused by the spatial variation of the gravitational potential; light traveling from deeper in the potential of a cluster is expected to be redshifted, compared to light originating from the outskirts of the cluster [1]. The GRS effect has the potential to constrain theories in which there are long-range non-gravitational forces acting on dark matter, modifying gravity on cluster scales [2]. The effect was first measured by Wojtak, Hansen & Hjorth (WHH) [3], a study which was subsequently repeated (with minor modifications) by Dominguez-Romero *et al.* [4].

WHH used 125k spectroscopic redshifts, taken from the seventh data release [5] of the Sloan Digital Sky Survey (SDSS) [6], matched to 7.8k clusters from the GMBCG cluster catalog [7]. They used the brightest cluster galaxies (BCGs) as a proxy for the centers of clusters. They assumed that, in general, BCGs have relatively small velocity dispersions compared to other bound galaxies, and reside close to the bottom of the gravitational potential. WHH divided their galaxy sample into four bins, based on the transverse distance between cluster-galaxies and respective BCGs, r_{gc} , extending up to 6 Mpc. In each bin, they calculated the line-of-sight velocity of galaxies in the rest-frame of the BCG,

$$v_{\text{gc}} = c \frac{z_{\text{gal}} - z_{\text{BCG}}}{1 + z_{\text{BCG}}}, \quad (1)$$

where z_{BCG} and z_{gal} respectively stand for the redshift of BCGs and of associated galaxies, and c is the speed of light. The stacked v_{gc} -distributions of galaxies from

the entire sample of clusters were fitted with a phenomenological model, using a Markov chain Monte Carlo (MCMC) program. The derived mean of the distributions was interpreted as the GRS signal. On average, cluster-galaxies were found to have a redshift difference relative to corresponding BCGs, amounting to a velocity difference, $\Delta v_{\text{gc}} \approx -7$ km/s.

WHH calculated the prediction for the signal from general relativity (GR), as well as from modified theories of gravity [8]. They first derived the GRS profile of a single cluster in the weak field limit,

$$\Delta_1(r_{\text{gc}}) = \frac{2}{c \Sigma(r_{\text{gc}})} \int_{r_{\text{gc}}}^{\infty} [\Phi(r) - \Phi(0)] \frac{\rho(r) r}{\sqrt{r^2 - r_{\text{gc}}^2}} dr, \quad (2)$$

where Φ is the gravitational potential, and ρ and Σ are respectively the three-dimensional and surface-density profiles of galaxies. They then convolved Δ_1 with the distribution of cluster masses in their sample, estimated from the observed velocity dispersion profile, using stacked NFW models [9].

Subsequent works, notably those of Zhao *et al.* [10] and of Kaiser [11], modified the theoretical prediction; these took into account effects such as the so-called transverse Doppler shift and surface brightness modulation. The added corrections were found to be of the same order of magnitude as the GRS signal, some inducing redshifts and some blueshifts. Summed together, the prediction of Kaiser is of a relatively flat dependence of Δv_{gc} on r_{gc} , with a mean value of -9 (GR only) or -12 km/s (GR and kinematic effects).

The purpose of this study is to revise the measurement of WHH. In the next sections we describe the analysis in detail, following up with our results and conclusions.

^{*} Iftach Sadeh, i.sadeh@ucl.ac.uk

[†] Low Lerh Feng, lerh.low.13@ucl.ac.uk

[‡] Ofer Lahav, o.lahav@ucl.ac.uk

METHODOLOGY

Dataset

We used spectroscopic redshifts derived from the tenth data release (DR10) [12] of the SDSS, including measurements taken with the Baryon Oscillation Spectroscopic Survey (BOSS) [13], occupying the redshift range, 0.05 to 0.6. We associated the DR10 data with galaxy clusters, using the catalog of Wen, Han & Liu (WHL) [14]. The WHL sample includes $\sim 130\text{k}$ clusters, detected using a friends-of-friends algorithm, based on photometric data. The virial radius of a cluster is commonly approximated by r_{200} , the radius within which the mean density of a cluster is 200 times that of the critical density of the universe [15]. The latter is additionally used to define m_{200} , the cluster mass within r_{200} . The WHL catalog is nearly complete for clusters with masses, $m_{200} > 2 \cdot 10^{14} M_{\odot}$, and redshifts, $z < 0.5$, and is $\sim 75\%$ complete for $m_{200} > 0.6 \cdot 10^{14} M_{\odot}$ and $z < 0.42$. Cluster mass is estimated using a scaling relation between mass and optical richness. The latter was estimated by WHL using x-ray or weak-lensing methods, and is given in Eq. 2 of [14]. The derived average cluster mass in our selected cluster sample is $m_{200} = 1.3 \cdot 10^{14} M_{\odot}$. This is commensurate with the mean value of cluster masses in the WHH dataset, $m_{200} = 1.6 \cdot 10^{14} M_{\odot}$, allowing us to directly compare the results of their measurement with our own.

In the initial stage of the analysis, the spectroscopic redshifts were subjected to various quality cuts, ensuring e.g., that the uncertainty on the redshift is below 10^{-4} , and that the confidence in the likelihood-fit of the redshift is high. We then matched galaxy spectra to BCG positions, keeping only those clusters for which the BCG had a corresponding spectrum. Additionally, each cluster had to contain at least one galaxy within transverse distance, $r_{\text{gc}} < 6$ Mpc, and velocity, $|v_{\text{gc}}| < 4,000$ km/s. Conversion from angular to physical distances was performed using a flat Λ CDM cosmology, with $\Omega_{\text{m}} = 0.307$ and the Hubble constant, $H_0 = 67.8 \text{ km s}^{-1} \text{ Mpc}^{-1}$ [16].

The initial selection left us with 31k clusters and 426k associated galaxies. Following the selection procedure discussed in the next section, we were left with 60k galaxies and 12k clusters, having $r_{\text{gc}} \lesssim 3$ Mpc. An additional 25k galaxies and 5k clusters were used for systematic checks.

Fitting procedure

WHH employed a MCMC program to fit the velocity distribution to the phenomenological model,

$$f(v_{\text{gc}}) = p_{\text{cl}} \cdot f_{\text{Gauss}}(v_{\text{gc}}) + (1 - p_{\text{cl}}) \cdot f_{\text{Lin}}(v_{\text{gc}}), \quad (3)$$

where f_{Gauss} is a convolution of two Gaussian distributions, having a common mean value, Δv_{gc} , and f_{Lin} is

a linear function. The quasi-Gaussian contribution represents galaxies bound to clusters. It accounts for the intrinsic non-Gaussianity of velocity distributions of individual clusters, and for the variation in cluster masses in the sample. The linear part of the model represents a uniform background of interlopers (line-of-sight galaxies which are not gravitationally bound to the cluster). The fraction of bound galaxies, p_{cl} , is a free parameter of the MCMC program, which is marginalized over, as are the two coefficients of f_{Lin} , the width of the two Gaussian functions, and the relative normalization of the two.

Scaling the separation between galaxies and associated BCGs by r_{200} takes advantage of the self-similarity of clusters; we therefore used r_{gc} -bins defined in units of r_{200} . We fitted the v_{gc} -distribution with Eq. 3 in each bin using **MultiNest**, a Bayesian inference tool employing importance nested sampling [17]. The fits for the various r_{gc} -bins were found to be compatible with the data, scoring better than 99% in K-S tests.

The observed velocity dispersions were of the order of several hundred km/s, more than 50 times larger than the GRS signal, Δv_{gc} . As the signal was difficult to confirm visually, we also computed the ratio between the integral of the negative and of the positive parts of the v_{gc} -distribution. The latter is a model-independent measure of the magnitude of the signal. It was shown to correlate well with the derived value of Δv_{gc} , validating that the **MultiNest** fitting procedure is not biased. In addition, we wrote a simple Metropolis-Hastings MCMC program and cross-checked the fit-results.

Sample composition and systematic tests

Our baseline dataset may be utilized in various ways to perform the measurement. One of the main sources of ambiguity is that we are interested in galaxies which are several Mpc away from the corresponding BCGs. On average, the distance between close pairs of clusters in our dataset corresponds to $2.3r_{200}$, where for the bulk of the cluster sample, $0.8 < r_{200} < 1.2$ Mpc. Many galaxies are therefore likely to be associated with multiple clusters, depending on their extent and separation.

We nominally define a pair of overlapping clusters as having a transverse separation, $r_{\text{cc}} < 4r_{200}$, and a velocity difference, $|v_{\text{cc}}| < 4,000$ km/s. We tested several galaxy selection schemes, with different restrictions on overlapping configurations. One possible selection procedure is to exclude all overlapping cluster pairs from the analysis. Another option is to exclude all but one member from any configuration of overlapping clusters. Alternatively, we may choose not to take into account cluster overlaps at all. We then accept only those galaxies that have only one cluster association, effectively performing exclusive selection on galaxies instead of on clusters.

In order to check the dependence of the signal on the composition of our dataset, we ran the analysis on sub-

sets of the data. Of these, tests involving BOSS-BCGs associated with SDSS galaxies revealed a systematic positive bias of a few km/s. So as to understand this effect, we define the quantity, $\delta m_r^{\text{gc}} = m_r^{\text{g}} - m_r^{\text{c}}$, where m_r^{c} and m_r^{g} respectively stand for the r -band magnitude of a BCG, and that of the brightest matched galaxy within one r_{200} of the BCG. Positive δm_r^{gc} values correspond to BCGs which are indeed found to be the brightest source within the area of a cluster. We observed on average, $\delta m_r^{\text{gc}} = -0.3$ for configurations in which the two surveys were mixed. The implication of this is that for this subsample, it is likely that BCGs were misidentified in the cluster catalog. As a result, selected BCGs were less likely to represent the bottom of the gravitational potential well of clusters, effectively suppressing the GRS signal. One should also keep in mind that the difference between SDSS and BOSS redshifts is almost an order of magnitude smaller than the uncertainties on the redshifts. It is therefore possible that the bias originates e.g., from changes made in the template-fitting procedure between data-releases.

Another important systematic is the treatment of clusters with high galaxies-multiplicities, which we denote by n_{gal} . These configurations are subject to two types of bias. The first is due to the fact that v_{gc} depends on the redshifts of both a galaxy and the corresponding BCG; consequently, an error in the redshift of a given BCG affects all matched galaxy-velocities in a correlated way. The second effect that we observed, was that the value of δm_r^{gc} , while generally positive, tends to decrease as n_{gal} increases. We, therefore, concluded that clusters become more susceptible to misidentification of the BCG with growing multiplicities. In order to mitigate these effects, we down-weighted the contribution of clusters with high multiplicities in the v_{gc} -distribution. We found that this change mainly affected the signal for low values of r_{gc} .

An additional possible source of bias is the uncertainty associated with individual spectroscopic redshifts. We checked that there was no correlation between these, and the corresponding values of v_{gc} .

RESULTS

We estimated Δv_{gc} using a sliding window for the transverse separation between galaxies and clusters. The sliding window nominally had a width of $0.5r_{200}$, and a step size of $0.1r_{200}$. For our primary selection, we elected to discard configurations in which SDSS and BOSS spectra were mixed together. This reduced the number of clusters and galaxies by 16% and 11%, respectively. We also excluded all overlapping cluster pairs, further reducing these numbers by a respective 34% and 46%. The final dataset was composed of 12600 clusters and 60626 matched galaxies. The measurement was restricted to transverse separation values below $2.5r_{200}$.

The reason for this last condition may be inferred from

Fig. 1(a). The figure shows the dependence on r_{gc} of the number of galaxies, n_{gal} , of the number of associated clusters, n_{clst} , and of the ratio, $n_{\text{gal}}/n_{\text{clst}}$. One may observe that for $r_{\text{gc}} < 1.3r_{200}$, the multiplicities of matched clusters and galaxies decrease; this is in accordance with the expected trend for the surface density of galaxies in clusters (see e.g., figure 8 in [18]). However, for $r_{\text{gc}} \gtrsim 2r_{200}$, both the multiplicities and the galaxy-to-cluster ratio increase. This comes about as galaxies at large r_{gc} have an increasingly higher probability of being associated with another cluster. Such configurations therefore tend to suppress the signal of the GRS, and should be rejected from the analysis.

The dependence of Δv_{gc} on r_{200} is presented in Fig. 1(b). We find that on average, $\Delta v_{\text{gc}} = -11_{-5}^{+7}$ km/s for $1 < r_{\text{gc}}/r_{200} < 2.5$, with uncertainties given as 1 standard deviation of the average signal. In physical scales, the measurement extends up to galaxy-cluster transverse separations of ~ 3 Mpc.

In addition to the primary result, we present a measurement with an increased r_{gc} -bin width. The two results are consistent within uncertainties. We note that the set-up with the wider bins has a radial resolution which is slightly too low to describe the GRS effect at low values of r_{gc} . On the other hand, for high r_{gc} -values, the increase in statistics in each bin seems to stabilize the result. Finally, we also include a measurement of Δv_{gc} , in which SDSS and BOSS spectra are used congruently. This change incurs a systematic shift of a few km/s, as discussed above.

The uncertainty on Δv_{gc} was derived from that on the `MultiNest` fit, combined with the variations incurred due to the following systematic checks: changing the minimal number of matched galaxies in a cluster between 1 and 7; not down-weighting clusters with high galaxy multiplicities; using different overlap-removal methods, as described above; changing the values of the cluster overlap parameters, using $3 < r_{\text{cc}}/r_{\text{gc}} < 5$ and $3000 < v_{\text{cc}} < 6000$ km/s; down-weighting galaxies with high spectroscopic redshift uncertainties; randomly excluding a fraction of galaxies or clusters of a given data sample. Of these, the dominant systematic variation originated from changing r_{cc} , the threshold for the transverse separation between clusters.

For comparison, Fig. 1(b) also shows the results of WHH within the region of interest. Our measurement is consistent with these, and has comparable uncertainty estimates. However, we note that the significance of our result is smaller than that of WHH, who quote a value, $\Delta v_{\text{gc}} = -7.7 \pm 3.0$ km/s. The reason for this is that WHH computed the integrated signal for all clusters within $r_{\text{gc}} < 6$ Mpc. They estimated the uncertainty from that of their MCMC model-fit, which was mainly determined by the size of their data sample. In the case of the current analysis, the uncertainty is driven by our systematic tests, rather than by the available number of clusters and galaxies. Considering these, and the limited

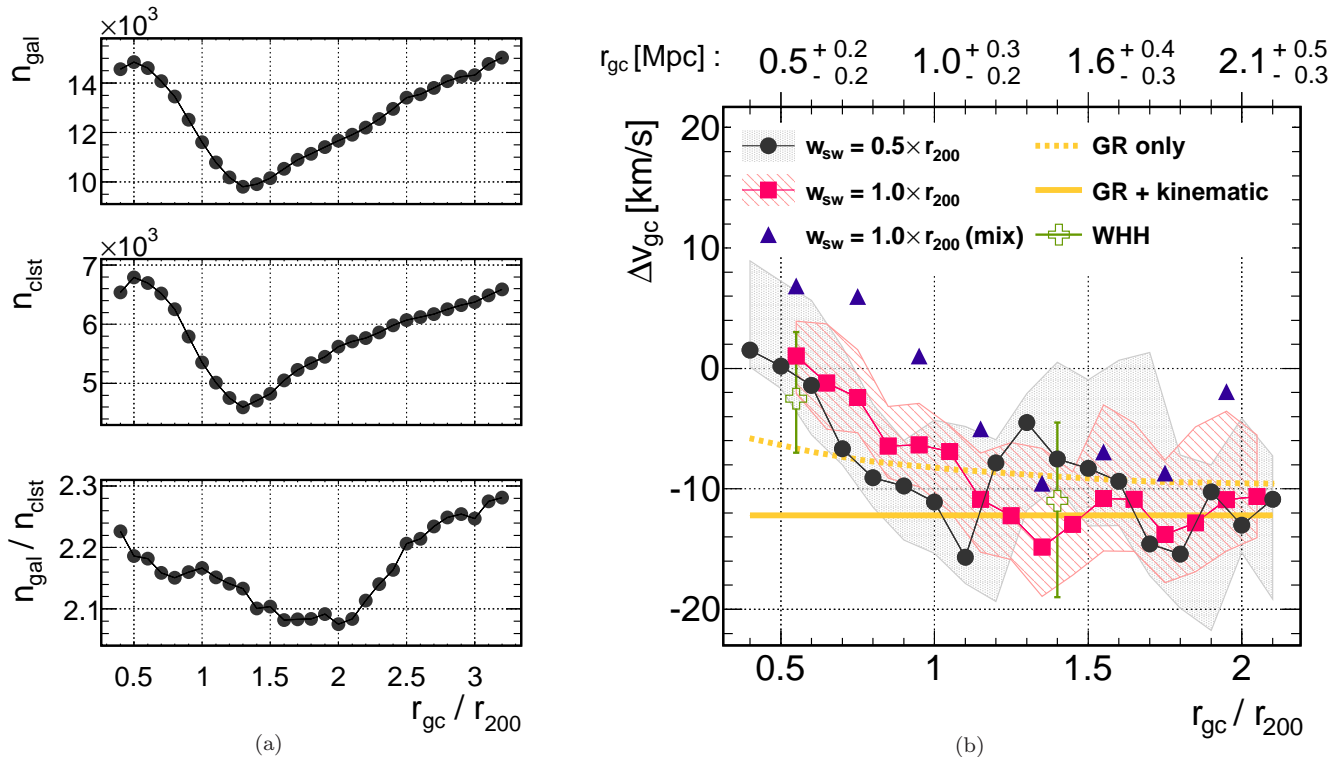


FIG. 1. (a): Dependence of the number of galaxies, n_{gal} , of the number of associated clusters, n_{clst} , and of the ratio, $n_{\text{gal}}/n_{\text{clst}}$, on the separation between BCGs and associated galaxies, r_{gc} . Bins of r_{gc} are defined by a sliding window with a width of $0.5r_{200}$, where each data-point is placed in the center-position of the corresponding bin. (b): Dependence of the signal of the GRS, Δv_{gc} , on r_{gc} , where the width of the sliding window is denoted by w_{sw} . The shaded areas around the two nominal results (circles and squares) correspond to the variations in the signal due to the systematic tests described in the text, combined with the uncertainty on the model-fit. On average, $\Delta v_{\text{gc}} = -11^{+7}_{-5}$ km/s for $1 < r_{\text{gc}}/r_{200} < 2.5$. The third dataset (triangles) includes configurations in which SDSS and BOSS redshifts are mixed together. The bold lines represent the GR predictions of Kaiser [11], with and without his added kinematic effects, as indicated; finally, the crosses represent the measurement of WHH. The top axis specifies the median value and the width of the distribution of r_{gc} (in Mpc) for four bins of width $0.5r_{200}$, centered at $(0.5, 1, 1.5 \text{ and } 2) r_{200}$.

range of acceptance in r_{gc} , our final relative uncertainty on Δv_{gc} is higher.

Calculating the GR prediction for Δv_{gc} is beyond the scope of this study. However, the range of cluster masses used in our analysis is comparable to that of the WHH sample. We therefore refer to the corresponding estimate of Kaiser of -9 (GR only) or -12 km/s (including kinematic effects) [11]. Our results are in good agreement with this prediction for $r_{\text{gc}} > r_{200}$, while at smaller values of r_{gc} , the profile of Δv_{gc} is steeper in the data. Additionally, we observe that it is not possible to distinguish between the GR predictions with and without the kinematic corrections.

SUMMARY

The gravitational redshift effect allows one to directly probe the gravitational potential in clusters of galaxies. As such, it provides a fundamental test of GR.

Following up on the analysis of Wojtak, Hansen & Hjorth, we present a new measurement with a larger

dataset. We use spectroscopic redshifts taken with the SDSS and BOSS, and match them to the BCGs of clusters from the catalog of Wen, Han & Liu. The analysis is based on extracting the GRS signal from the distribution of the velocities of galaxies in the rest frame of corresponding BCGs. We focus on optimizing the selection procedure of clusters and of galaxies, and take into account multiple possible sources of systematic biases not considered by WHH.

We find an average redshift of -11 km/s with a standard deviation of $+7$ and -5 km/s for $1 < r_{\text{gc}}/r_{200} < 2.5$. The result is consistent with the measurement of WHH. However, our overall systematic uncertainty is relatively larger than that of WHH, mainly due to overlapping cluster configurations; the significance of detecting the GRS signal in the current analysis is therefore reduced in comparison. Our measurement is in good agreement with the GR predictions. Considering the current uncertainties, we can not distinguish between the baseline GR effect and the recently proposed kinematic modifications.

With the advent of future spectroscopic surveys, such as Euclid and DESI [19], we will have access to larger,

more homogeneous datasets. We expect that the new spectra will help to reduce the systematic uncertainties on the measurement, though dedicated target selection may be required. Additionally, new data will facilitate novel techniques of detecting the GRS signal, such as the cross-correlation method suggested in [20].

ACKNOWLEDGEMENTS

We would like to thank Jacob Bekenstein, Jens Hjorth, Pablo Jimeno, Nick Kaiser, John Peacock, David Schlegel and Radek Wojtak, for the useful discussions regarding the nature of spectroscopic redshifts, galaxy clusters and GRS.

O.L. acknowledges an Advanced European Research Council Grant, which supports the postdoctoral fellowship of I.S.

This work uses publicly available data from the SDSS. Funding for SDSS-III has been provided by the Alfred P. Sloan Foundation, the Participating Institutions, the National Science Foundation, and the U.S. Department of Energy Office of Science. The SDSS-III website is <http://www.sdss3.org/>.

-
- [1] Y.-R. Kim and R. A. C. Croft, *ApJ* **607**, 164 (2004), [astro-ph/0402047](#); L. Nottale, *A&A* **118**, 85 (1983); A. Cappi, *ibid.* **301**, 6 (1995).
- [2] J. M. Gelb, B.-A. Gradwohl, and J. A. Frieman, *ApJ* **403**, L5 (1993), [hep-ph/9208239](#); S. S. Gubser and P. J. E. Peebles, *Phys. Rev. D* **70**, 123511 (2004), [hep-th/0407097](#); J. A. Keselman, A. Nusser, and P. J. E. Peebles, *Phys. Rev. D* **81**, 063521 (2010), [arXiv:0912.4177 \[astro-ph.CO\]](#); G. R. Farrar and R. A. Rosen, *Phys. Rev. Lett.* **98**, 171302 (2007), [astro-ph/0610298](#).
- [3] R. Wojtak, S. H. Hansen, and J. Hjorth, *Nature* **477**, 567 (2011), [arXiv:1109.6571 \[astro-ph.CO\]](#).
- [4] M. J. d. L. Domínguez-Romero, D. Garca Lambas, and H. Muriel, *MNRAS* **427**, L6 (2012).
- [5] K. N. Abazajian *et al.* (SDSS Collaboration), *ApJS* **182**, 543 (2009), [arXiv:0812.0649 \[astro-ph\]](#).
- [6] D. J. Eisenstein *et al.*, *AJ* **142**, 72 (2011), [arXiv:1101.1529 \[astro-ph.IM\]](#).
- [7] J. Hao *et al.*, *ApJS* **191**, 254 (2010), [arXiv:1010.5503 \[astro-ph.CO\]](#).
- [8] S. M. Carroll, V. Duvvuri, M. Trodden, and M. S. Turner, *Phys. Rev. D* **70**, 043528 (2004), [astro-ph/0306438](#); M. Milgrom, *ApJ* **270**, 365 (1983); J. D. Bekenstein, *Phys. Rev. D* **70**, 083509 (2004), [astro-ph/0403694](#).
- [9] J. F. Navarro, C. S. Frenk, and S. D. M. White, *ApJ* **490**, 493 (1997), [astro-ph/9611107](#).
- [10] H. S. Zhao, J. A. Peacock, and B. Li, *Phys. Rev. D* **88**, 043013 (2013), [arXiv:1206.5032 \[astro-ph.CO\]](#).
- [11] N. Kaiser, *MNRAS* **435**, 1278 (2013), [arXiv:1303.3663 \[astro-ph.CO\]](#).
- [12] C. P. Ahn *et al.*, *ApJS* **211**, 17 (2014), [arXiv:1307.7735 \[astro-ph.IM\]](#).
- [13] K. S. Dawson *et al.*, *AJ* **145**, 10 (2013), [arXiv:1208.0022 \[astro-ph.CO\]](#).
- [14] Z. L. Wen, J. L. Han, and F. S. Liu, *ApJS* **199**, 34 (2012), [arXiv:1202.6424 \[astro-ph.CO\]](#).
- [15] P. Peebles, *Principles of Physical Cosmology*, Princeton series in physics (Princeton University Press, 1993); J. Peacock, *Cosmological Physics*, Cambridge Astrophysics (Cambridge University Press, 1999).
- [16] Planck Collaboration, P. A. R. Ade, N. Aghanim, C. Armitage-Caplan, M. Arnaud, M. Ashdown, F. Atrio-Barandela, J. Aumont, C. Baccigalupi, A. J. Banday, *et al.*, *A&A* **571**, A16 (2014), [arXiv:1303.5076 \[astro-ph.CO\]](#).
- [17] F. Feroz, M. P. Hobson, and M. Bridges, *MNRAS* **398**, 1601 (2009), [arXiv:0809.3437](#); F. Feroz and M. P. Hobson, *MNRAS* **384**, 449 (2008), [arXiv:0704.3704](#); F. Feroz, M. P. Hobson, E. Cameron, and A. N. Pettitt, (2013), [arXiv:1306.2144 \[astro-ph.IM\]](#).
- [18] S. M. Hansen, T. A. McKay, R. H. Wechsler, J. Annis, E. S. Sheldon, and A. Kimball, *ApJ* **633**, 122 (2005), [astro-ph/0410467](#).
- [19] R. Laureijs *et al.*, (2011), [arXiv:1110.3193 \[astro-ph.CO\]](#); The Dark Energy Spectroscopic Instrument (DESI), “<http://desi.lbl.gov/>,” (2014).
- [20] R. A. C. Croft, *MNRAS* **434**, 3008 (2013), [arXiv:1304.4124 \[astro-ph.CO\]](#).